Journal of Power Sources 245 (2014) 95–100

Contents lists available at SciVerse ScienceDirect

Journal of Power Sources

journal homepage: www.elsevier.com/locate/jpowsour

Polyvinyl formal based gel polymer electrolyte prepared using initiator free in-situ thermal polymerization method

Hong-yan Guan [a,b], Fang Lian [a,*], Kai Xi [b], Yan Ren [a], Jia-lin Sun [a], R. Vasant Kumar [b]

[a] School of Materials Science and Engineering, University of Science and Technology Beijing, Beijing 100083, China
[b] Department of Materials Science and Metallurgy, University of Cambridge, Cambridge, CB2 3QZ, UK

HIGHLIGHTS

- A novel polyvinyl formal (PVFM) based gel polymer electrolyte (GPE) was prepared via in-situ thermal polymerization.
- It is the first time to report the PVFM based electrolyte for Li-ion batteries.
- Its conductivity at ambient temperature is $\sim 10^{-3}$ S cm^{-1}.
- Its electrochemical stability window is 1.5–5 V *vs.* *Li/Li*$^{+}$.
- The polymerization mechanism is investigated by FTIR analysis.

ARTICLE INFO

Article history:
Received 7 April 2013
Received in revised form
5 June 2013
Accepted 20 June 2013
Available online 28 June 2013

Keywords:
Polyvinyl formal
Initiator free
Thermal polymerization
Gel polymer electrolyte
Lithium-ion batteries

ABSTRACT

Novel polyvinyl formal (PVFM) based gel polymer electrolytes (GPEs) are developed using an initiator free thermal polymerization method. The polymerization mechanism during the cross-linking process is investigated by means of Fourier transform infrared (FTIR) spectroscopy measurements. With the prepared GPEs (containing 2 to 5 wt % PVFM), Li polymer batteries with $LiFePO_4$ as the cathode are assembled, and the electrochemical properties such as interfacial impedance, electrochemical stability window and cycling performance are evaluated. The resulting PVFM based GPEs present a better thermal stability compared with the corresponding conventional liquid electrolyte and an acceptable conductivity of $\sim 10^{-3}$ S cm^{-1} at ambient temperatures. Cyclic voltammetric (CV) curves reveal that the electrochemical stability window of PVFM based GPE is 1.5–5V *vs.* *Li/Li*$^{+}$ and wider than that for the corresponding liquid electrolyte which is 1.8–4.4 V. The discharge capacity of the polymer Li/$LiFePO_4$ battery is 145 mAh g^{-1} over a voltage range of 2.5–4.25 V at 1/10 C rate after 80 cycles with a small capacity fade.

1. Introduction

Safety issues in a lithium-ion battery using a liquid electrolyte, arising from leakage and potential combustion of organic liquids , are of primary concern in their practical applications especially in hybrid electric vehicles (HEVs) and plug-in hybrids (PHEVs) [1,2]. In the past decades, many safer alternatives to liquid electrolytes have been investigated, and gel polymer electrolytes (GPEs), which possess both cohesive properties of a solid electrolyte and diffusive properties of a liquid electrolyte, have been attracting increasing attention [3–9]. The present GPEs for lithium-ion batteries reported are usually based on the polymer matrix as specified in the following list: poly (ethylene oxide) (PEO), poly (vinylidene fluoride)-hexafluoropropylene (PVdF-HFP), polyacrylonitrile (PAN), poly (methyl methacrylate) (PMMA), and polyvinyl chloride (PVC) [10]. Despite offering safer and flexible packaging alternatives to liquid electrolytes, the present GPEs are plagued with various problems. For example, the PEO based electrolytes offer low ionic conductivity; PAN based electrolytes, although exhibiting a relatively high conductivity and a wide electrochemical stability window, are known to readily passivate upon contact with the lithium metal anode; and the plasticized PMMA based electrolytes show poor mechanical strength [11]. The high dielectric constant of the P (VdF-HFP) polymers and the presence of electron withdrawing fluorine atoms are advantageous factors for dissociating lithium salts to form lithium ions in the redox reactions, however, the formation of stable LiF and >C=CF– unsaturated bonds may not

* Corresponding author. No. 30, Xueyuan Road, Haidian District, Beijing 100083, China. Tel./fax: +86 (10) 82377985.
E-mail addresses: lianfang@mater.ustb.edu.cn, ustbenergy@yahoo.cn (F. Lian).

0378-7753/$ – see front matter © 2013 Elsevier B.V. All rights reserved.
http://dx.doi.org/10.1016/j.jpowsour.2013.06.120

only deteriorate the battery performance but also raise safety concerns due to thermal runway arising from the highly exothermic reactions [12]. In order to overcome these problems, several new kinds of polymer gels are being considered in the field of GPEs.

Polyvinyl acetal based GPEs have been extensively studied for use in nickel-metal hydride batteries [13,14]; the presence of −OH groups are considered as the source of hydrogen bonding which assist in the formation of the polymer gel [15]. Polyvinyl acetal has been used as a suitable polymer matrix in lithium-ion batteries because of high conductivity, unique film-forming properties, and in particular, excellent adhesion on many surfaces [16–18]. In previous studies, polyvinyl acetal based GPEs are usually reported to be formed by a solution casting method, in which polymers are dissolved in a dilute solvent to form a film by volatilization. The low-boiling solvent in the electrolytic solution could volatilize easily from the dilute solvent, leading to difficulty for achieving good ionic conductivity.

Inoue et al. [19] have proposed the use of suitable side groups to build up polymeric networks or molecules with interesting properties. In this study, PVFM with tri-functional groups (vinyl formal, vinyl hydroxyl and vinyl acetate) is chosen as the matrix, as they are expected to form stable polymeric electrolytes with high mechanical strength, good flexibility, and high conductivity. The basic chemical structure of PVFM is shown in Fig. 1. The C═O bond in the side chains of PVFM can interact with the oxygen atoms in plasticizers and thus exhibit good compatibility with the electrolyte solution. As reported by Saito et al. [20], the −OH group is a strong Lewis base thus attracting lithium ions, thereby affecting the cation mobility in a manner similar to that of the oxygen sites in ether in polyethylene oxide (PEO).

According to previous studies [21,22], chemical cross-linking is a dominant method in forming an irreversible gel. The exact details depend upon the use of cross-linking agents and initiators, however, the by-products generated from the initiators, such as oxygen, nitrogen and other reactive radicals may degrade the performance of the lithium polymer batteries. Furthermore, most gel electrolytes show poor wettability for electrodes and poor penetration because of their high viscosity and incomplete formation. In this work, the PVFM based GPE was synthesized by thermal polymerization of a mixed solution of PVFM and a $LiPF_6$ based liquid electrolyte, without the use of any thermal initiator. The gelling process is shown in Fig. 2. The in-situ thermal polymerization can help improve the interfacial contact between the electrolyte and the electrode through direct transformation from a liquid precursor solution filling the porous electrode to a gel. Thus, gel formation by in-situ cross-linking reaction at a low temperature without using a polymerization initiator should be considered as an important breakthrough for the preparation of GPEs.

2. Experimental

2.1. Preparation of gel polymer electrolytes

Polyvinyl formal (PVFM) with a molecular weight of 70,000 was obtained from *Johnson Controls*. A weakly polar CO group is rigidly

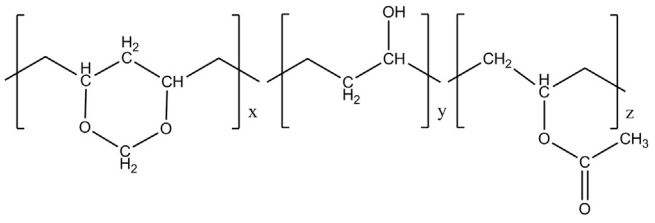

Fig. 1. Molecular structure of polyvinyl formal.

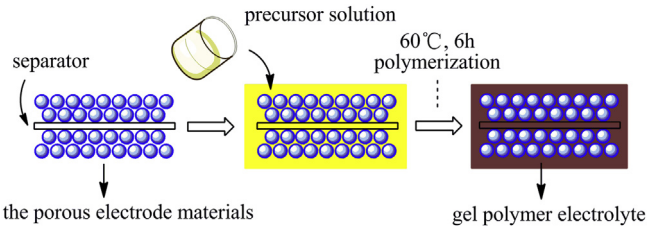

Fig. 2. Schematic diagram depicting transformation from liquid into a gel electrolyte.

attached to the non-polar main chain as shown in Fig. 1. The percentage of ether linkages and hydroxyl groups are both vital parameters for determining the solubility of PVFM in organic solvents on one hand and the extent of polymerization on the other. The molar percentages of vinyl acetal, vinyl hydroxyl and vinyl acetate groups used are 62.3%, 10.5%, and 27.2%, respectively while the degree of acetalization is 92.2%.

For the preparation of the GPEs, PVFM was used without any further purification. Liquid electrolyte consisting of 1M $LiPF_6$ dissolved in the solvent ethylene carbonate (EC): dimethyl carbonate (DMC) = 3:7 (V/V) was purchased from Beijing Institute of Chemical Reagent. The precursor solution was prepared by dissolving a certain selected amount (2%, 3%, 4% or 5% by weight) of PVFM in the liquid electrolyte. According to the Hansen solubility parameters, PVFM can be dissolved in EC: DMC = 3:7 (V/V) mixture solvent to form a homogenous solution. After stirring in an argon filled glove box for about 30 min, the solution mixture was placed in a sealed container and transferred into a thermostat maintained at 60 °C where it was held for 6 h in order to carry out the cross-linking reaction of polyvinyl formal. Finally, the GPEs were formed which were found to be effective for tethering liquid components and binding the battery parts, such as the separator and the porous electrodes.

2.2. Electrode preparation and battery assembly

For the electrochemical studies, $LiFePO_4$ based cathode plates were prepared by coating a slurry consisting of $LiFePO_4$, acetylene black and poly (vinylidenefluoride) (PVdF) in N-methyl pyrrolidone (NMP) as the binder in the ratio of 80:15:5 by weight, on an aluminum foil by the doctor blade process. The thickness of the electrode ranged from 40 to 50 μm after doctor blade coating, followed by mechanical pressing. A number of 2032-type coin cells Li/$LiFePO_4$ were assembled with tri-layer PP/PE/PP (Ube) as the separator and precursor solutions with different content of PVFM prepared as described in Section 2.1. The batteries were then placed in the thermostat at 60 °C for 6 h to achieve polymerization. For comparison, a liquid electrolyte based coin cell was also assembled. All the batteries were assembled in a glove box filled with Ar, and O_2 and H_2O < 0.5ppm.

2.3. Measurements

The conductivity of GPEs was measured by a conductivity meter (*Shanghai Leici, DDSJ-308A, China*). Thermogravimetric analysis (TGA) and differential scanning calorimetry (DSC) data were collected through a NETZSCH STA449F3 analyzer (*Germany*) from room temperature to 400 °C at a heating rate of 10 °C min^{-1} in argon atmosphere. FTIR spectra were recorded on NEXUS FT-IR670 spectrometer (*USA*) in the range of 400–4000 cm^{-1}.

The electrochemical stability windows of the electrolytes were measured by means of cyclic voltammetry (CV) on an electrochemical work station (*Chi660a, Shanghai, China*) equipped with a

three-electrode cell (working electrode : steel (Φ = 1.6 cm), counter electrode: steel, and reference electrode: Li^+/Li). Interfacial impedance measurement was performed using the same electrochemical work station (*Chi660a, Shanghai, China*) over frequency range of 100 kHz to 0.01 Hz at an amplitude of 5 mV applied potential. Cycling charge and discharge tests for the batteries were conducted at room temperature over a voltage range of 2.5–4.25 V at 1/10 C rate (corresponding to 0.14 mA cm^{-2}) for 80 cycles using Land Battery Test System (*Wuhan Land Electronic Co. Ltd., China*).

3. Results and discussion

3.1. Visual observation of GPEs

In order to ascertain the self-standing properties of GPEs, precursor solutions with 2, 3, 4 and 5 wt. % of PVFM were prepared in glass containers and marked as GPE2, GPE3, GPE4 and GPE5, respectively. After the cross-linking treatment in the thermostat at 60 °C for 6 h, free-standing gels were obtained. The summary from the visual observation of GPEs is listed in Table 1. Basically, there were some visible liquid residues on the walls of the glass containers for GPE2 and GPE3, which indicates that the addition of 2 and 3 wt. % PVFM is not sufficient to achieve liquid-free gel. It is believed that liquid residues were not caused by incomplete cross-linking but because the liquid content was higher than the absorbing capacity of the polymer framework, thus extruding the extra liquid during the formation of the polymer network.

3.2. Conductivity test

Temperature dependence of the conductivities of the GPEs with different amounts of PVFM ranged from 0 to 60 °C is shown in Fig. 3. As expected, the conductivities of the electrolytes decrease linearly with the reciprocal temperature (1000 T^{-1}) regardless of the content of PVFM, and the conductivity-temperature relationship of GPEs obey the Vogel–Tammann–Fulcher (VTF) equation. The conductivities obtained for GPE2, GPE3, GPE4, and GPE5 at 25 °C are 9.82, 9.16, 8.82 and 8.67 mS cm^{-1}, respectively. Compared with the value of 12.22 mS cm^{-1} for the pure liquid electrolyte at 25 °C, the conductivities of the GPEs are respectable and can be seen to decrease slightly at the higher polymer fraction. It is generally understood that the conductive cation species move in a continuous conduction path formed by the solvent domain surrounding the polymer skeleton. The Lewis basic –OH polar site is considered to enhance the local viscosity of the GPE and induce a reduction of the mobility of the conductive species [20], thus contributing to a minor decrease in the conductivity. The Arrhenius activation energy calculated from the linear region in Fig. 3 is listed in Table 2. The activation energy values of GPEs generally increases with PVFM concentration (although the difference between 3 and 4% PVFM samples is negligible) in the temperature range as tested, and the ionic mobility of GPEs decreases with increasing PVFM content. The decrease in ionic mobility is caused by an increase of migration resistance. Consequently, with the increase of PVFM content, the interactions between solvated lithium ions and polymer are enhanced and the conductivity is correspondingly decreased.

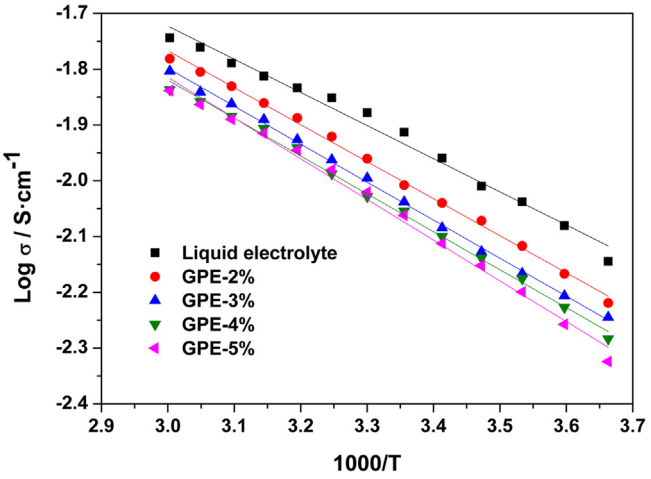

Fig. 3. Conductivities and the fitted results of the liquid electrolyte and gel polymer electrolytes. The liquid electrolyte used is 1.0 M $LiPF_6$ in EC: DMC = 3:7 (Vol).

However, the conductivity of PVFM based GPEs is higher than most of the GPEs reported in the literature [4].

3.3. Thermal stability

Thermal stability is critical for GPEs to maintain the macroscopic physical network that can prevent the liquid solvents from evaporating at high temperatures [23]. In this research, GPE4 was chosen for thermal analysis by thermogravimetric analysis (TGA) and differential scanning calorimetry (DSC) measurements under an argon atmosphere, and the results were compared with those for the PVFM and liquid electrolyte. The results are shown in Fig. 4. Fig. 4a shows that glass transition temperature of PVFM is at 110.45 °C; and the exothermic peak at 145.62 °C represents the crystallization peak of PVFM, consistent with the fact that heat is evolved when the uncrystallized polymer chain segments in PVFM are crystallized. It can be observed from Fig. 4b and c that both the liquid electrolyte and GPE4 show weight loss within the temperature range of 179 ~ 206 °C. At around 200 °C the weight loss for the liquid electrolyte is 45 wt. % while it is lower at 37 wt % for the sample GPE4. In liquid electrolyte the calculated weight percent of the various components - $LiPF_6$ salt, DMC (with a boiling point of 90 °C) and EC (with a boiling point of 238 °C) – are 11.75, 57.58 and 30.66 wt. %, respectively. Consequently, the weight loss at 179 ~ 206 °C can be almost fully attributed to the evaporation of DMC. Meanwhile, DSC data exhibits a maximum endothermic peak of 0.81 mW mg^{-1} for the liquid electrolyte, while for the GPE electrolyte the peak is relatively much lower at 0.019 mW mg^{-1}, which is in good accordance with the TGA results. Additionally, the exothermic peak at 152.6 °C in Fig. 4c is closely related to the crystallization of uncrystallized polymer chain segments in PVFM, and also the interaction between PVFM and liquid electrolyte. Therefore, the thermal stability of the electrolyte is shown to improve with the introduction of PVFM matrix, attributed to the three-dimensional polymer network formed in GPE and the high adhesion property of PVFM which can help block evaporation of the liquid components.

Table 1
Visual observation of GPEs.

PVFM content [wt. %]	2	3	4	5
Sample	GPE2	GPE3	GPE4	GPE5
Free-standing	yes	yes	yes	yes
Liquid residue	yes	trace	no	no

Table 2
Activation energy for ionic conductivity of GPEs with different concentrations of PVFM.

PVFM concentration [wt. %]	0	2	3	4	5
Activation energy [kJ mol^{-1}]	4.96	5.52	5.66	5.65	6.07

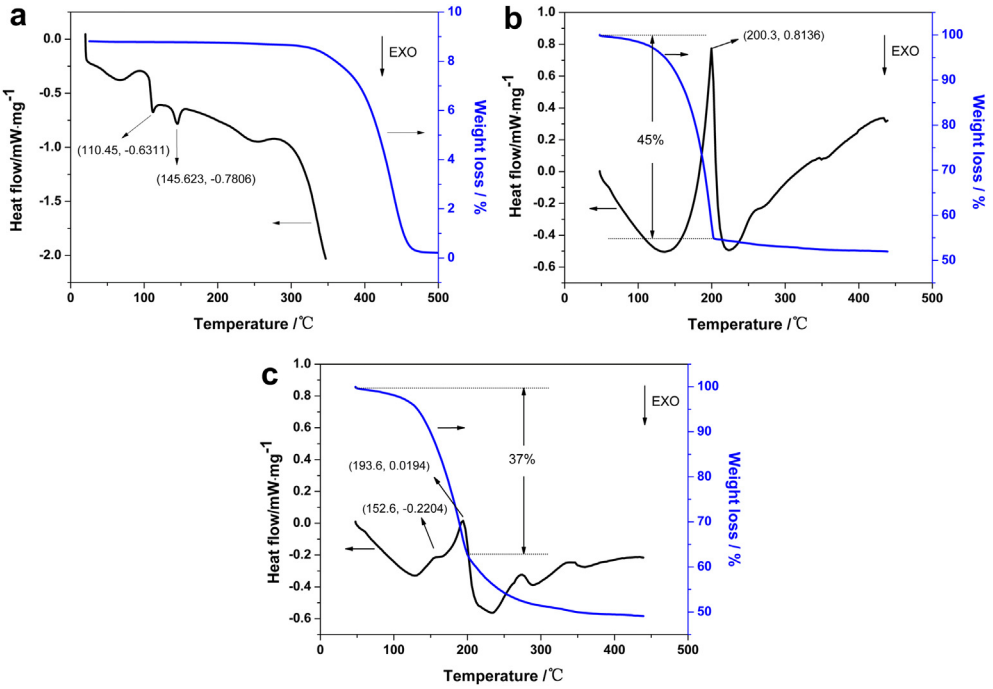

Fig. 4. TGA-DSC analysis of the PVFM (a), liquid electrolyte (b) and the GPE4 (c) under argon atmosphere at a scanning rate of 10 °C min^{-1}. Labels in the thermal scans represent (T in °C, ΔH in mW mg^{-1}) values at the peak positions.

3.4. FTIR spectroscopy

Fig. 5 shows the FTIR spectra of PVFM, liquid electrolyte and GPE4, measurements being conducted at the ambient temperature to help understand the possible polymerization mechanism of PVFM based GPE. In order to gain an insight into the specific interaction among functional groups, the changes of groups are carefully analyzed and summarized as follows. In PVFM, peaks at 1020, 1070, 1135, and 1180 cm^{-1} represent the C—O—C—O—C bond in the ether ring. According to the reports of W. Choi et al. [24] and V. Etacheri et al. [1], in liquid electrolyte the peaks at 1484 and 1405 cm^{-1} represent the interaction between EC and PF_6^- anions; the peaks at 1197, 1081 and 847 cm^{-1} correspond to the C═O groups of EC, C—O groups of EC and PF_6^- anions, respectively. The peaks at 1020 and 1135 cm^{-1} cannot be observed in GPE4 when compared with PVFM,

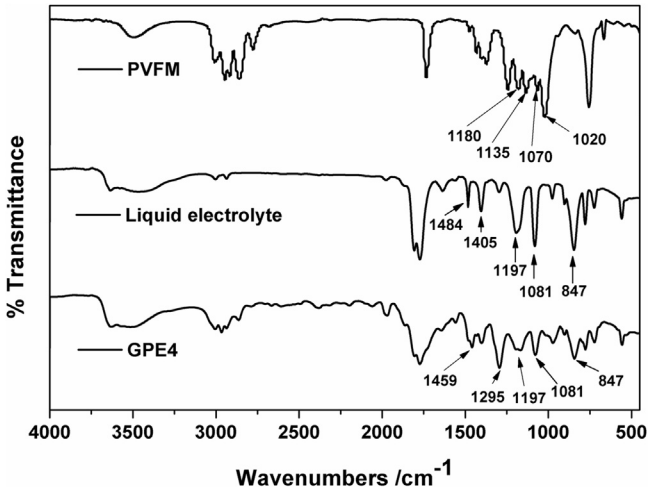

Fig. 5. FTIR spectra of PVFM, liquid electrolyte and GPE4.

suggesting the cleavage of the ether rings in PVFM molecular structure. And the possible sites of broken bonds are shown in Fig. 6. Compared with liquid electrolyte, GPE4 exhibits weaker peak at 1405 cm^{-1} and no obvious peak at 1484 cm^{-1}, which is contributed to the reduced interaction between EC and PF_6^- anions due to the introduction of PVFM; however, peak at 847 cm^{-1} in GPE4 decreased obviously, implying that part of PF_6^- anions participated in the polymerization process as catalyst most possibly. The peaks at 1081 and 1197 cm^{-1} in GPE4 result from the EC component of liquid electrolyte. The appearance of the new peak at 1459 cm^{-1} in GPE4 represents the enhancement of shear bending vibration of–CH_2, which suggests that the –CH_2 groups in the main chain is extended significantly thus confirming polymerization. Additionally, according to the report of N.S. Choi et al. [25], the new strong peak at 1295 cm^{-1} in GPE4 represents the C—O—C stretching in the host polymer interacting with Li^+ ions.

Combining above analysis and previous reports from Aoki [26] and Allcock [27], we proposed the polymerization process of PVFM based GPE. As shown in Fig. 6, the ether linkage bonds in the vinyl acetal groups of PVFM break down under attack from the strong Lewis acid PF_5, which are generated by the slight decomposition of PF_6^-. The scission of C—O bonds when bonded to the methylene groups results in the formation of oxyradicals and methylene radicals. On the other hand, the scission of C—O bonds when bonded to the polymer chain results in the formation of hydroperoxide and methyne radicals. Then the produced radicals crosslink with each other to form new C—O—C bonds in polymer skeleton. In conclusion, for a PVFM based GPE system, under the effect of PF_5 the cleavage of the acetal ring and the cross-linking of produced radicals contribute to the polymerization process.

3.5. The electrochemical stability window

Fig. 7 represents the cyclic voltammetry curves for cells with both the liquid electrolyte and GPE4 based electrolyte using lithium as the reference electrode, at a scanning rate of 5 mV·s^{-1}. As shown

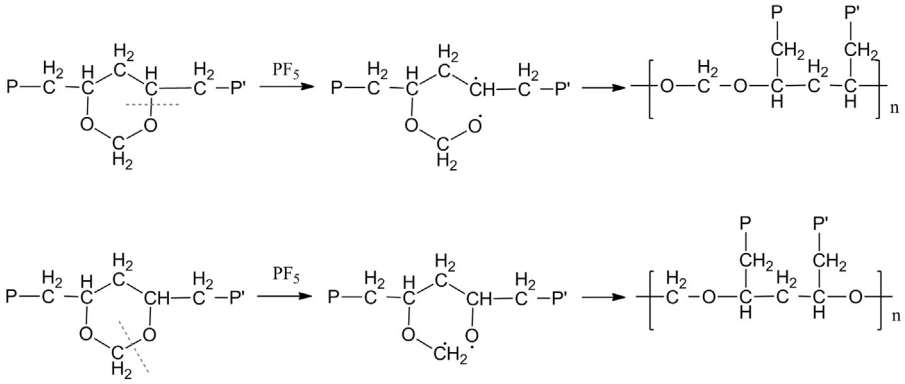

Note: P and P' represent other functional groups except the ether ring in the main chain.

Fig. 6. Schematic representation of the polymerization mechanism of the PVFM based GPE.

in Fig. 7a for the liquid electrolyte, a large decomposition current of 1.17 mA·cm^{-2} can be observed in the first cycle from 1.8 to 0 V, which represents the electrochemical reduction of solvents [1,28]. The oxidation reaction peak is observed from 4.4 to 5 V, which implies that the liquid electrolyte can be used only between 1.8 and 4.4 V *vs. Li/Li*$^+$. As for the GPE electrolyte as demonstrated in Fig. 7b, the reductive decomposition occurs below 1.5 V in the initial cycle with a lower current density of 0.84 mA·cm^{-2}. Additionally, on sweeping toward more positive potentials, the electrochemical stability has been extended to 5.0 V. In the subsequent cycles, the cyclic voltammetry curves show the process of redox reactions to be reversible in the GPE. Besides, the current density is gradually decreased, which is attributed to the formation of a passive layer on the SS electrode. This suggests that the PVFM based GPE can effectively suppress the decomposition by electrochemical reduction and oxidation of the solvent over a wider electrochemical stability window ranging from 1.5 to 5 V *vs. Li/Li*$^+$. It is therefore a very promising candidate for application as a gel polymer electrolyte in a lithium-ion battery.

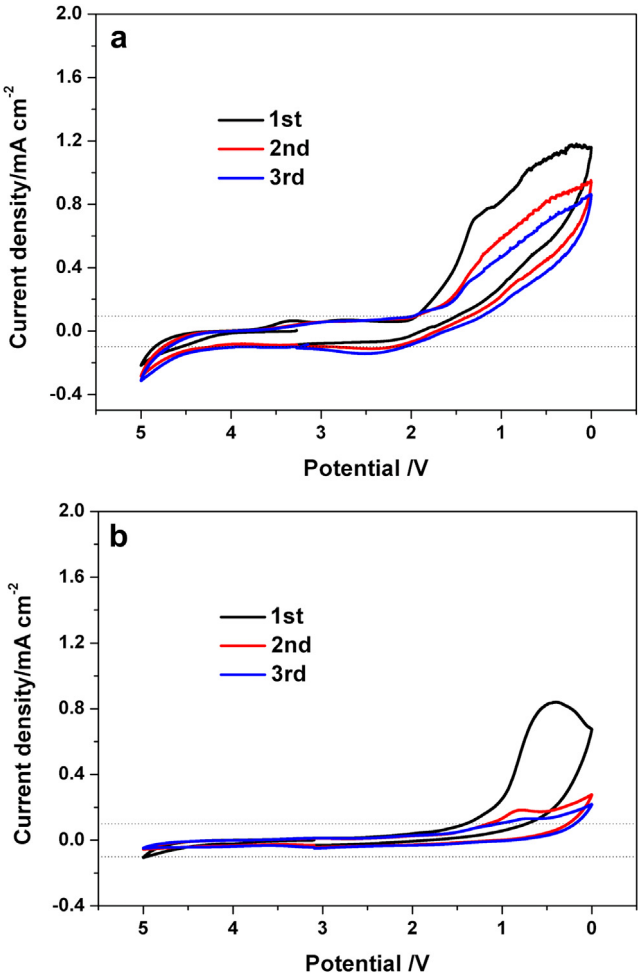

Fig. 7. Cyclic voltammetry of the liquid electrolyte (a) and the GPE4 (b) on stainless steel at a scan rate of 5 mV s^{-1}.

3.6. AC impedance spectra

To study the interfacial resistance behavior, the Li/LiFePO$_4$ batteries based on both the liquid electrolyte and the GPEs were first slowly charged and discharged between 2.5 V and 4.25 V at a constant current of C/10 (~0.08 mA) for 3 cycles, then charged to a constant voltage of 3.7 V for impedance measurement. Fig. 8 shows the a.c. impedance results for the Li/LiFePO$_4$ batteries at 3.7 V with the different electrolytes, and the median frequency arc represents the interfacial impedance between the electrode surface and the electrolyte [22]. It can be seen that the interfacial impedance of

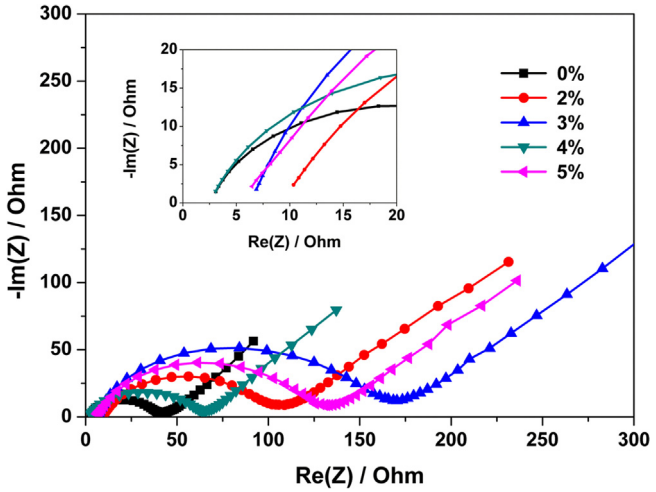

Fig. 8. AC Impedance spectra at room temperature of batteries assembled with the liquid electrolyte and the GPEs (2–5% PVFM).

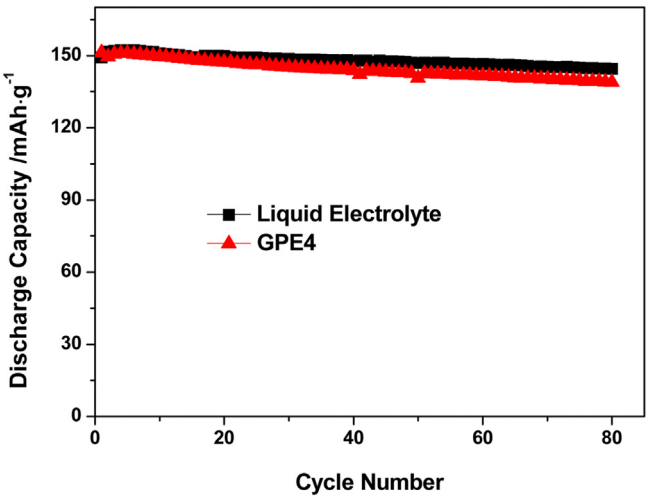

Fig. 9. Cycle performance of Li/$LiFePO_4$ cells at a current of C/10 at ambient temperature. The liquid electrolyte used is 1M $LiPF_6$ in EC: DMC (3:7, in Vol).

battery assembled with liquid electrolyte (0% PVFM) is about 40 Ω cm^2 and the batteries assembled with GPEs exhibit interfacial resistances of more than 64 Ω cm^2. The interfacial impedance of batteries assembled with GPEs does not simply monotonically change with the polymer fraction but the behavior appears random. As shown, a minimum interfacial resistance of about 64 Ω cm^2 is exhibited by cells based on GPE4. The interfacial behavior of batteries may be attributable to a combination of factors namely - the polymer structure, the network morphology, the formation of Lewis basic site in the three-dimensional network, and the contact between electrode and the electrolyte. It is reasonable to expect that cells based on the GPEs will show a lower conductivity and a higher interfacial impedance than those based on a liquid electrolyte, a small price worth paying for much improved safety.

3.7. Cycling performance

Li/$LiFePO_4$ coin cells were constructed to investigate the application of the PVFM based GPE in lithium-ion batteries. The cells were studied using charge/discharge battery testing method at C/10 rate between 2.5 and 4.25 V. Fig. 9 shows the cycling performance of cells assembled with both the liquid electrolyte and GPE4, subjected to 80 cycles. Both cells exhibit a reversible capacities of >145 mAh g^{-1}. The cell assembled with GPE4 exhibits a slightly lower reversible initial capacity and cycling stability than with the liquid electrolyte, arising primarily from the higher interfacial impedance.

4. Conclusions

Homogenous mixture solutions of PVFM and the liquid electrolyte 1M $LiPF_6$/EC: DMC = 3:7 (V/V) are successfully turned into a self-standing gel after a thermal treatment without employing any thermal initiator. The GPE4 sample containing 4% of PVFM exhibits an acceptable conductivity of 8.82 mS cm^{-1} at 25 °C; meanwhile, GPE4 reveals better thermal stability compared with the liquid electrolyte arising from the blocking action of the three-dimensional polymer network. FTIR results indicate that the polymerization occurs through the interaction between C—O—C bonds, which arise from the breaking of ether linkage bonds in PVFM, and the strong Lewis acid PF_5 generated by the slight decomposition of the $LiPF_6$ salt. The cyclic voltammetry results show that the electrochemical stability of GPE4 is excellent within the 1.5–5 V range *vs. Li/Li*$^+$ improving upon the 1.8–4.4 V range for the liquid electrolyte. A Li/$LiFePO_4$ battery comprising the GPE shows a larger interfacial resistance in comparison with a battery based on the liquid electrolyte thus accounting for some of the lowering of the discharge capacity. It is believed that the decrease in the mobility of the cations can be attributed to the interaction between solvated lithium ions and Lewis base —OH polar sites in PVFM. Overall, a Li-ion battery using the new gel polymer electrolyte is a promising way forward to achieve enlarged electrochemical window and improved safety.

Acknowledgments

This work was financially supported by Johnson Controls Battery Group, INC. and the Fundamental Research Funds for the Central Universities (No. FRF-MP-12-005B). Thanks to Prof. Weihua Qiu of USTB for fruitful discussion and USTB for the award of a scholarship to Hongyan Guan for 6 months visit at University of Cambridge.

Appendix A. Supplementary data

Supplementary data related to this article can be found at http://dx.doi.org/10.1016/j.jpowsour.2013.06.120.

References

[1] V. Etacheri, R. Marom, R. Elazari, G. Salitra, D. Aurbach, Energy Environ. Sci. 4 (2011) 3243–3262.
[2] G.N. Zhu, Y.G. Wang, Y.Y. Xia, Energy Environ. Sci. 5 (2012) 6652–6667.
[3] K.E. Aifantis, S.A. Hackney, R.V. Kumar, High Energy Density Lithium Batteries, Wiley–VCH, Weinham, 2010.
[4] J.W. Fergus, J. Power Sources 195 (2010) 4554–4569.
[5] Y.H. Liao, X.P. Li, C.H. Fu, R. Xu, M.M. Rao, L. Zhou, S.J. Hu, W.S. Li, J. Power Sources 196 (2011) 6723–6728.
[6] J.L. Li, C. Daniel, D. Wood, J. Power Sources 196 (2011) 2452–2460.
[7] N.H. Idris, M.M. Rahman, J.Z. Wang, H.K. Liu, J. Power Sources 201 (2012) 294–300.
[8] M.H. Ryou, Y.M. Lee, K.Y. Cho, G.B. Han, J.N. Lee, D.J. Lee, J.W. Choi, J.K. Park, Electrochim. Acta 60 (2012) 23–30.
[9] M.Z. Kufian, M.F. Aziz, M.F. Shukur, A.S. Rahim, N.E. Ariffin, N.E.A. Shuhaimi, S.R. Majid, R. Yahya, A.K. Arof, Solid State Ionics 208 (2012) 36–42.
[10] A.M. Stephan, Eur. Polym. J. 42 (2006) 21–42.
[11] A.M. Stephan, K.S. Nahm, Polymer 47 (2006) 5952–5964.
[12] P. Raghavan, J. Manuel, X.H. Zhao, D.S. Kim, J.H. Ahn, J. Power Sources 196 (2011) 6742–6749.
[13] C.C. Yun, Mater. Lett. 58 (2003) 33–38.
[14] J.L. Qiao, J. Fu, R. Lin, J.X. Ma, J.S. Liu, Polymer 51 (2010) 4850–4859.
[15] P.B. Bhargav, V.M. Mohan, A.K. Sharma, V. Rao, Ionics 13 (2007) 441–446.
[16] M. Ulaganathan, S.S. Pethaiah, S. Rajendran, Mater. Chem. Phys. 129 (2011) 471–476.
[17] S. Rajendran, V.S. Bama, M.R. Prabhu, Ionics 16 (2010) 27–32.
[18] Y.W. Li, J.W. Wang, J.W. Tang, Y.P. Liu, Y.D. He, J. Power Sources 187 (2009) 305–311.
[19] K. Inoue, T. Itaya, Bull. Chem. Soc. Ipn 74 (2001) 1381–1395.
[20] Y. Saito, M. Okano, K. Kubota, T. Sakai, J. Fujioka, T. Kawakami, J. Phys. Chem. B 116 (2012) 10089–10097.
[21] H. Li, X.T. Ma, J.L. Shi, Z.K. Yao, B.K. Zhu, L.P. Zhu, Electrochim. Acta 56 (2011) 2641–2647.
[22] Z.H. Chen, L.Z. Zhang, R. West, K. Amine, Electrochim. Acta 53 (2008) 3262–3266.
[23] B. Beak, F. Xu, C. Jung, Solid State Ionics 202 (2011) 40–44.
[24] W. Choi, J.Y. Lee, B.H. Jung, H.S. Lim, J. Power Sources 136 (2004) 154–159.
[25] N.S. Choi, J.K. Park, Solid State Ionics 180 (2009) 1204–1208.
[26] H. Aoki, M. Uehara, T. Suzuki, A. Yoshida, Eur. Polym. J. 16 (1980) 577–581.
[27] H.R. Allcock, F.W. Lampe, J.E. Mark, Contemporary Polymer Chemistry, third ed., Prentice Hall, 2003.
[28] D. Aurbach, Y. Talyosef, B. Markovsky, E. Markevich, E. Zinigrad, L. Asraf, J.S. Gnanaraj, H.J. Kim, Electrochim. Acta 50 (2004) 247–254.